

TECHNICAL ADVANCE

Velocity of climate change algorithms for guiding conservation and management

ANDREAS HAMANN¹, DAVID R. ROBERTS¹, QUINN E. BARBER¹, CARLOS CARROLL² and SCOTT E. NIELSEN¹¹Department of Renewable Resources, Faculty of Agricultural, Life, and Environmental Sciences, University of Alberta, 751 General Services Building, Edmonton, AB, T6G 2H1, Canada, ²Klamath Center for Conservation Research, PO Box 104, Orleans, CA, 95556, USA

Abstract

The velocity of climate change is an elegant analytical concept that can be used to evaluate the exposure of organisms to climate change. In essence, one divides the rate of climate change by the rate of spatial climate variability to obtain a speed at which species must migrate over the surface of the earth to maintain constant climate conditions. However, to apply the algorithm for conservation and management purposes, additional information is needed to improve realism at local scales. For example, destination information is needed to ensure that vectors describing speed and direction of required migration do not point toward a climatic *cul-de-sac* by pointing beyond mountain tops. Here, we present an analytical approach that conforms to standard velocity algorithms if climate equivalents are nearby. Otherwise, the algorithm extends the search for climate refugia, which can be expanded to search for multivariate climate matches. With source and destination information available, forward and backward velocities can be calculated allowing useful inferences about conservation of species (present-to-future velocities) and management of species populations (future-to-present velocities).

Keywords: assisted migration, climate change adaptation, climate change vulnerability, conservation, no-analogue climates

Received 23 May 2014; revised version received 19 August 2014 and accepted 4 September 2014

Introduction

The velocity of climate change is a climatic landscape metric proposed by Loarie *et al.* (2009) that evaluates the exposure of organisms in the landscape to climate change. The measure is derived by dividing the rate of projected climate change in units of °C per year by the rate of spatial climate variability, i.e. the temperature differential of adjacent grid cells, measured in °C km⁻¹. The division cancels the °C units, while units of kilometre in the denominator and the units of year in the numerator swap positions. The resulting variable is a speed or velocity measured in units of kilometres per year, and represents an initial rate at which species must migrate over the surface of the earth to maintain constant climate conditions.

One advantage of this approach is its simplicity and clarity of interpretation. No biological response of organisms to climate change is implicitly or explicitly inferred as, for example, would be by projections based on species distribution models. Rather, velocities are a simple function of spatial and temporal variation in climate conditions in a particular landscape, and can be

interpreted as one of several risk factors that contribute to persistence or loss of species and populations in complex landscapes under climate change. The measure has been used to rank exposure of organisms to climate change in the 5th assessment report of the Intergovernmental Panel on Climate Change (IPCC, 2014; fig. SPM 5.), to evaluate the integrity of protected area systems under climate change (Ackerly *et al.*, 2010; Schueler *et al.*, 2014), to describe the expected rate and direction of climate migrants (Dobrowski *et al.*, 2013; Burrows *et al.*, 2014), and to identify climate refugia during glacial–interglacial cycles (Sandel *et al.*, 2011).

Limitations of the approach have been pointed out by Loarie *et al.* (2009) and subsequent studies. Migration requirements inferred by velocity algorithms can be markedly different from the results of climate envelope approaches that attempt to match current and future climate regions (Corlett & Westcott, 2013; Diefenbaugh & Field, 2013; Ordonez & Williams, 2013). Climate velocity vectors can diverge in direction and magnitude among variables, and they are not easily combined into a multivariate measure of climate change exposure (Dobrowski *et al.*, 2013). Finally, scale and related search radius problems can arise in velocity calculations. In areas of flat terrain, velocity estimates may be inflated (approaching infinity in flat terrain),

Correspondence: Andreas Hamann, tel. (780) 492-6429, fax (780) 492-4323, e-mail: andreas.hamann@ualberta.ca

although suitable climate habitat may be very close, but just outside the search radius. Conversely, in mountainous terrain true migration requirements may be underestimated by orders of magnitude. For instance, a population near a mountain top may face extinction of suitable climate habitat in the immediate surroundings under climate change (a climatic *cul-de-sac*). Yet, the velocity algorithm will imply low migration requirements as long as the population is situated on a steep climatic slope.

To apply the velocity of climate change concept to conservation planning and natural resource management, three improvements are needed. First, a broader search radius of the velocity algorithm and destination information should ensure that vectors describing speed and direction do not point toward climatic *cul-de-sacs* or result in infinite velocities. Instead, infinite velocities should indicate no-analogue climate conditions within the entire study area. Second, the algorithm should be expanded from a univariate temperature analysis to more appropriately assess a suite of biologically relevant climate variables. Third, with source and destination information available, forward and backward velocities from current climate locations to potential future climate space, and from projected future climate cells back to matching current locations should be estimated. While this might seem equivalent at first sight, the two calculations yield profoundly different results and both measures allow useful inferences for the management and conservation of species and their populations. Here, we provide a simple, easy to understand set of algorithms for the open-source R programming environment, capable of searching large datasets for univariate or multivariate climate matches and estimates of climate change velocities.

Materials and methods

Climate data

All climate data representing current, past, and future periods were generated with the ClimateWNA software package (Wang *et al.*, 2012; Hamann *et al.*, 2013), which is available for anonymous download (<http://www.ualberta.ca/~ahamann/climate.html> and <http://adaptwest.databasin.org/pages/adaptwest-climatewna>). The software overlays historical data and general circulation model (GCM) projections on high-resolution climate normal data and applies lapse-rate-based elevation adjustments, when resampling to different grid resolutions and projections. Climate surfaces were generated in Lambert Conformal Conic projection at 1 km resolution, and include various biologically relevant temperature and precipitation variables, as well as extremes, growing and chilling degree days, various dryness and indices and growing season descriptors such as frost-free days.

To represent current climate conditions, we use the 1961–1990 climate normal period. Future climate data for the 2011–2040, 2041–2070, and 2071–2100 period, hereafter referred to as the 2020s, 2050s, and 2080s, were based on A2 emissions scenarios implemented by seven GCMs of the CMIP3 multi-model dataset: CCMA CGCM3.1, CSIRO MK3.0, IPSL CM4, MIROC3.2 HIRES, MPI ECHAM5, NCAR CCSM3.0, UKMO HADGEM1, referenced in the IPCC's Fourth Assessment Report (IPCC, 2007). Similar to Fordham *et al.* (2011) we excluded poorly validated GCMs, and report ensemble velocity estimates based on individual runs for each future scenario.

Velocity algorithms

Given enough precision in measurement of climate variables, no two grid cells have the same climate value. Therefore, the search algorithm for finding a climate match for a current grid cell in a climate surface representing a future projection relies on a user-defined threshold. The search algorithm is implemented with the following R code

```
1 id <- 1:length(p)
2 for (i in 1:length(p)) {
3   ti <- id[abs(f-p[i])<t]
4   di <- sqrt((x[ti]-x[i])^2+(y[ti]-y[i])^2)
5   d[i] <- min(di) }
```

The variables p , f , x , y are vectors (or columns of a table), representing present (p) and future (f) climate values and their x and y coordinates in a gridded dataset. $p[i]$ denotes the i -th element in the vector. Line 1 creates a string of consecutive identification numbers, and line 2 initiates a processing loop for all present climate values. Line 3 extracts the identification numbers of future climate grid cells within a user-defined climate threshold (t) of a present climate reference cell ($p[i]$), Line 4 calculates the geographic distance of x and y coordinates of all matching future climate cells ($x[ti]$, $y[ti]$) to the present reference cell ($x[i]$, $y[i]$), and line 5 finds the shortest geographic distance (d) from this vector of distances to matching cells (di). This distance divided by the number of years between the current and future climate is the required velocity of migration.

The algorithm can be modified to process large datasets more than an order of magnitude faster by implementing thresholds through rounding and then working with lists of unique values

```
1 p <- round(p*t)/t; f <- round(f*t)/t
2 u <- unique(p)[order(unique(p))]
3 match <- function(u){c(which(u==f))}
4 m <- sapply(u, match)
5 for (i in 1:length(p)) {
6   mi <- m[which(u==p[i])]
7   d[i] <- sqrt(min((x[i]-x[mi])^2+(y[i]-y[mi])^2)}
```

Line 1 rounds present climate values (p) and future climate cells (f) using a user defined threshold (t) as above. Line 2 creates a list of unique present climate values after rounding, so the geographic search will only be carried out once for each unique climate value. Line 3 creates a function that we can

subsequently use to find all climate cells in the future dataset that match a current climate grid cell. Line 4 executes that function, creating a list of future climate matches for each unique present climate value. Line 5 initiates a processing loop as before. Line 6 now simply recalls the climate matches, and line 7 calculates as before the distance to the geographically closest climate match.

This computational approach also lends itself to a multivariate extension. Instead of creating a list of unique values for one climate variable, we can create lists of unique combinations of two or more climate variables

```
1 p1 <- round(p1*t1)/t1; f1 <- round(f1*t1)/t1
2 p2 <- round(p2*t2)/t2; f2 <- round(f2*t2)/t2
3 u <- unique(paste(p1,p2)); f <- paste(f1,f2)
```

Line 1 and 2 create lists of rounded climate values for two climate variables in present ($p1$, $p2$) and the equivalent for the future climate grids ($f1$, $f2$). In line 3 the two variables are combined into list of unique present climate value combinations (u) that can be searched for matches for the same combinations in the future grid (f). The remaining programme is identical to the above lines 3–7.

Sample code and sample datasets for all three algorithms can be found in online supplements: univariate threshold-based (Appendix S1), the faster approach with univariate lists of unique values (Appendix S2), and the multivariate extension (Appendix S3). In Appendix S3 we also use a k -nearest neighbour search algorithm, increasing computational efficiency by another order of magnitude. The appendices further include code for import of gridded climate surfaces, post-

processing of velocity grids, flagging of no-analogue climates, and tabular output of source and target coordinates of climate matches for further analysis of expected rate and direction of climate migrants.

Multivariate climate velocities

For a multivariate implementation of climate change velocities, we used a principal component analysis for a pooled sample of present and future climate surfaces. Climate variables for the principal component analysis include: mean annual temperature, mean temperature of the warmest month, mean temperature of the coldest month, mean annual precipitation, mean growing season (May to August) precipitation, annual compound moisture index, summer (June–August) compound moisture index, degree days above 5 °C, and number of frost-free days. Using principal component scores rather than original variables has the advantage that multiple highly correlated climate variables do not have an inappropriate influence the final velocity measure.

As variables $p1$ and $p2$ in the algorithm above, we use the first two principal component scores for each grid cell, which capture a large portion of the variance contained in the original climate variables. We further use a single threshold value for all components that yielded approximately 120 unique values for the first principal component score. Subsequent components (as long as principal component analysis is based on the eigenvalue decomposition of the correlation matrix) are therefore automatically weighted according to the variance

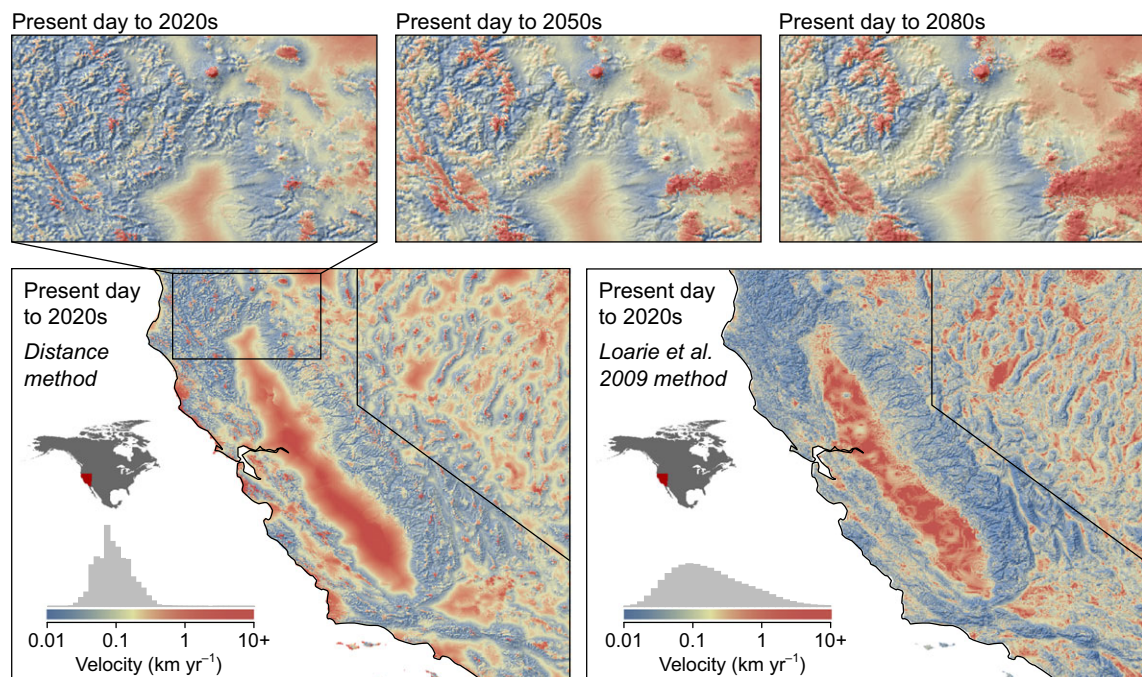


Fig. 1 The new distance-based velocity algorithm (left and top insets), and the standard slope method according to Loarie *et al.* (2009) compared. The velocity based on the distance to the nearest climate match yields lower velocities in flat areas, such as the central California valley (compare histograms). However, higher velocities are generated at mountain tops, where current climate conditions become locally extinct as climate change becomes more pronounced over time (top insets).

they explain. The number of 120 multivariate climate bins was empirically determined as described in the next section.

Results & discussion

Comparison of velocity algorithms

Estimates of velocity of required migration from a global search for climate equivalents broadly conform to the results of Loarie *et al.*'s (2009) standard velocity algorithm when climate equivalents are nearby. This generally applies under moderate climate warming scenarios or projections for the near future, such as the 2020s (Fig. 1). However, even by the 2020s, the required migration rates diverge near mountain tops, where the distance-based required migration rates are higher because they measure to a climate match further north or on an adjacent mountain with higher elevation positions. Conversely, our velocity estimates tend to be lower in valley bottoms, where geographic distances are measured to the base of the nearest mountain, while the standard velocity estimates can approach infinity if the surrounding grid cells are of the same elevation, and therefore show little or no spatial climate gradients (Fig. 1, histograms).

When calculated for a larger geographic region of western North America (25–80°N latitude and 100–179°W longitude), velocities obtained by the standard slope method and the proposed distance-based method are almost identical between the 5th and 95th percentile for a moderate degree of climate change (Table 1, first two data lines). However, for the 2050s and the 2080s,

Table 1 Distribution of climate change velocities for western North America for different time period and methods

| Time period & method | Velocity for percentiles | | | | |
|-------------------------|--------------------------|------|------|------|-------|
| | p5 | p25 | p50 | p75 | p95 |
| Mean annual temperature | | | | | |
| Slope method | | | | | |
| 6190 to 2050s | 0.05 | 0.17 | 0.53 | 1.64 | 2.83 |
| Climate match (forward) | | | | | |
| 6190 to 2020s | 0.05 | 0.15 | 0.47 | 1.61 | 3.33 |
| 6190 to 2050s | 0.08 | 0.26 | 0.75 | 2.54 | 6.12 |
| 6190 to 2080s | 0.10 | 0.34 | 0.94 | 2.88 | 7.39 |
| Multivariate (PCA) | | | | | |
| Climate match (forward) | | | | | |
| 6190 to 2020s | 0.21 | 0.77 | 1.87 | 3.55 | 9.87 |
| 6190 to 2050s | 0.40 | 1.36 | 2.81 | 4.96 | 10.68 |
| 6190 to 2080s | 0.52 | 1.61 | 3.29 | 5.54 | 10.67 |
| Climate match (reverse) | | | | | |
| 2020s to 6190 | 0.23 | 1.04 | 2.55 | 4.57 | 9.11 |
| 2050s to 6190 | 0.39 | 1.50 | 3.29 | 5.21 | 8.76 |
| 2080s to 6190 | 0.72 | 2.31 | 4.24 | 6.21 | 9.83 |

they diverge with the distance-based method yielding increasingly higher migration requirements than the standard slope method. Note that the slope method generally yields the same result regardless of the future time period as long as the rate of change measured in degree Celsius per year stays approximately constant. We therefore only included the 2050s values for comparison for the slope method in Table 1. Con-

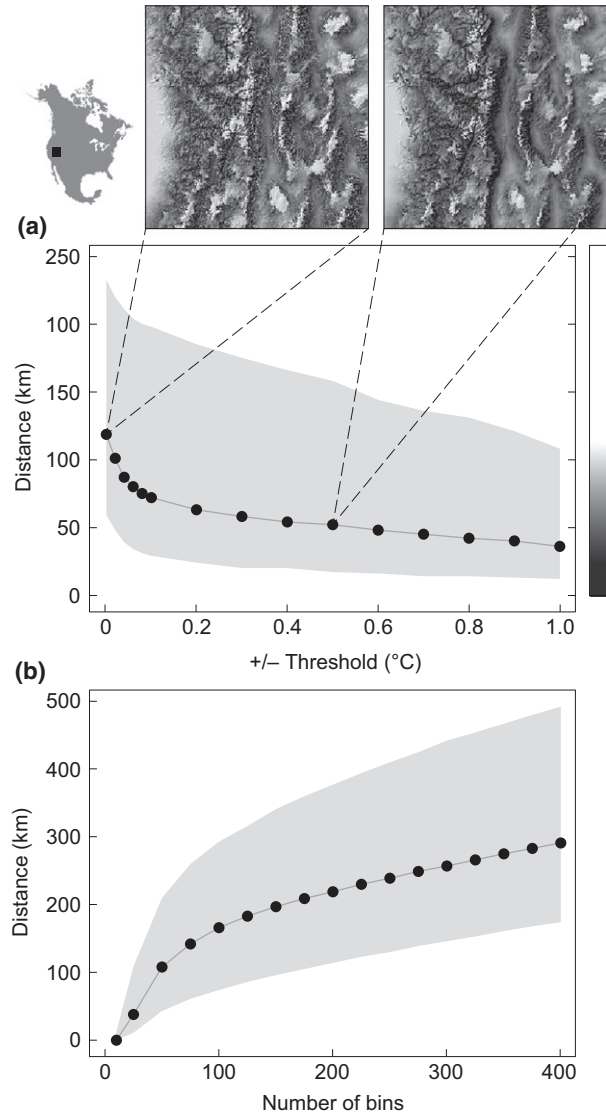


Fig. 2 Sensitivity of the distance-based velocity to the threshold value used to define a climate match (a). If the requested precision for a climate match becomes very high, geographic distances to a match increase rapidly, and the resulting velocity maps become noisy. For the multivariate implementation (b), high requested precision (high number of bins of unique climate combinations) does not have the same effect. However, the frequency of no-analogue climates increases rapidly (data not shown). Grey envelopes indicate the 25th and 75th percentiles of velocities for western North America.

versely, the required migration estimates from the distance-based method is strongly influenced by the absolute values of climate change, reflecting the increasing prevalence of climatic *cul-de-sacs* in the landscape as climate change progresses.

Sensitivity of threshold values and scale dependencies

An important decision for the implementation of the distance-based velocity algorithm is the threshold of what constitutes a matching climate between a current cell and a nearby grid cell that has a similar value in the future. Given enough precision in measurements, no two grid cells will have the same climate value, and this becomes obvious when matching cells in multivariate climate space. This decision could be informed by biological data, for example, if the climate tolerances of an organism are known. However, for a general landscape analysis we find it useful to set the threshold as small as possible while avoiding artefacts due to using excessive precision (Fig. 2a).

Generally, the required migration distances increase linearly and monotonically with smaller thresholds, but beyond a certain point velocities increase rapidly driven by more random climate matches. For example, if the algorithm has to search for a climate match to a present cell with a value of 5.36 °C, and the value of a nearby future climate cell of 5.32 °C is rejected, then large and small distances start to occur by random chance and the resulting surfaces become noisy (Fig. 2a, left inset). In the example shown in Fig. 2, a good threshold would be ± 0.2 °C. The resulting maps of velocity equal or

higher to this value remain very robust, until the threshold exceeds the warming signal so that the required migration distance is by definition zero.

Another factor that influences the velocity estimates, and that depends on user choices is the spatial resolution of the gridded climate data. For both Loarie's slope method and the distance-based method proposed in this paper, median velocities increase in the same monotonic fashion (Fig. 3). Maximum velocities for the distance-based method are not resolution dependent, while they decrease substantially for the slope-based method. The decrease in the slope-based method arises from the fact that at coarser resolutions it becomes less likely that surrounding cells all have the same elevation and temperature values, and therefore yield very high velocity estimates. Conversely, the distance-based method shows stronger resolution dependence for the minimum distance. This is due to the minimum velocity value being restricted by the distance to the nearest neighbour grid cell. We therefore recommend use of gridded data with as high resolution as is computationally feasible and justifiable based on the precision of interpolated climate grids.

Multivariate velocity calculations

Principal component analysis of multiple climate variable grids in western North America yielded two dimensions that explained 69% and 21% of the total variance for a cumulative total of 90% for the two climate dimensions (Table 2). The first component (PC1) represents temperature variables, with the highest eigenvectors for annual and summer temperature

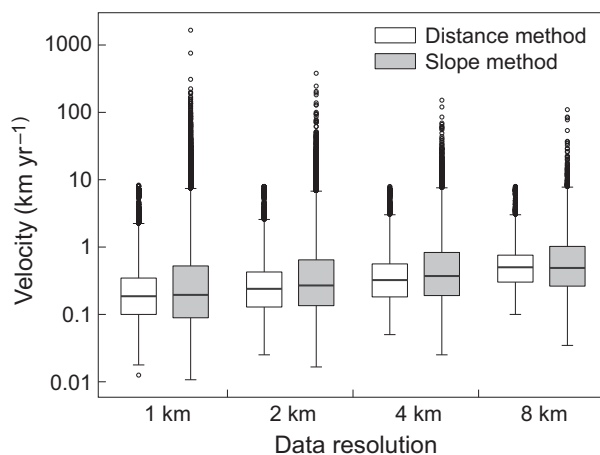


Fig. 3 Resolution sensitivity of the new distance vs. the standard slope method, corresponding to the California extent of Fig. 1. Both methods show identical median velocity increases as resolution becomes coarser. For the distance method, minimum velocities are by definition restricted by the size of grid cells.

Table 2 Loadings or eigenvalues of principal component scores for a pooled sample of present and future climate surfaces. The first two principal components are the basis for the velocity maps shown in Fig. 4

| Climate variable | PC1 | PC2 | PC3 |
|--|-------|------|-------|
| Mean annual temperature | 0.37 | 0.26 | -0.04 |
| Mean temperature of the warmest month | 0.38 | 0.08 | 0.16 |
| Mean temperature of the coldest month | 0.34 | 0.33 | -0.23 |
| Mean annual precipitation | -0.19 | 0.61 | -0.31 |
| Mean summer (May–August) precipitation | -0.21 | 0.51 | 0.75 |
| Annual compound moisture index | -0.34 | 0.29 | -0.45 |
| Summer (June–August) compound moisture index | -0.37 | 0.18 | 0.11 |
| Degree days above 5 °C | 0.38 | 0.14 | 0.17 |
| Number of frost-free days | 0.36 | 0.24 | -0.14 |

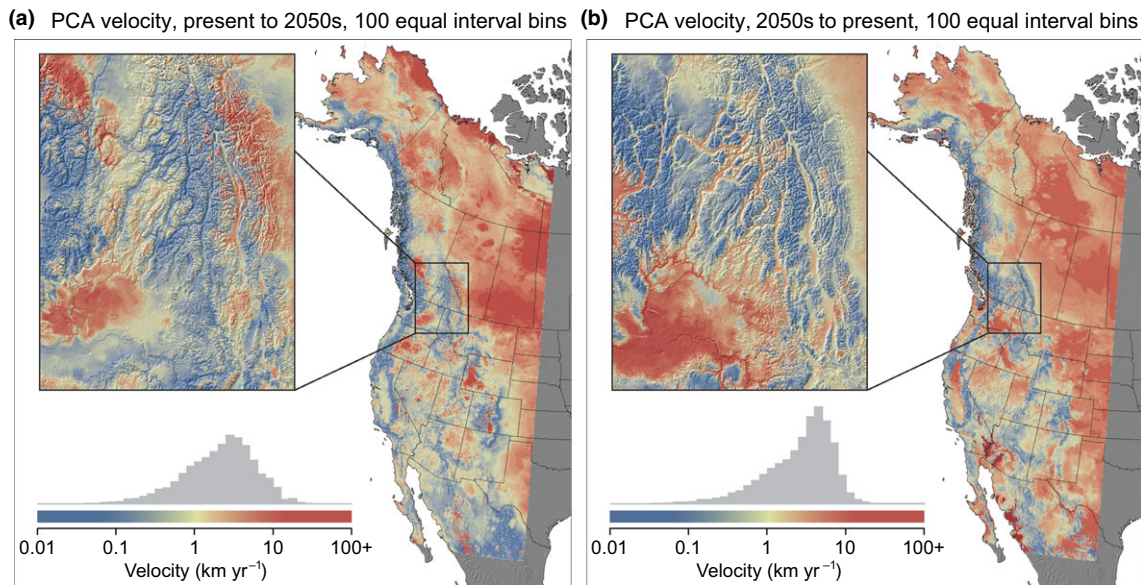


Fig. 4 Multivariate forward (a) vs. backward (b) velocity calculations from current to projected future climate conditions and vice versa. No analogue climates are indicated in dark red. The forward calculation can be interpreted as exposure of species and populations to climate change. The backward calculations can be used to prioritize need for human intervention, such as assisted migration prescriptions.

variables (Table 1, PC1). The second component (PC2) primarily represents mean annual precipitation, but also scores high for variables that describe mild winters. The third component (PC3) represents variance in summer precipitation that is not already captured by the second component. However, this additional component only explained 5% of the variance and for computational efficiency PC3 was not used in subsequent velocity calculations.

Estimates of velocity of climate change based on a multivariate climate matches of the first two principal components are shown in Fig. 4a, with additional statistics reported in Table 1. Velocities based on a multivariate climate match are always higher than the univariate estimate, which is expected since additional criteria were added to what constitutes a climate match. Adding more principal component dimensions would further increase velocity estimates across the distribution of values (data not shown). Otherwise, univariate and multivariate velocity estimates behave similarly, with a stronger climate change signal resulting in disproportionately higher velocities due to the increasing prevalence of climatic *cul-de-sacs* in the landscape (compare data lines 2–4 with 5–7 in Table 1).

The multivariate velocity algorithm behaves slightly differently than the univariate algorithm in one other respect. The lack of a climate match in a future surface to a present cell is rare in the univariate analyses, while no-analogue situations occur more frequently with

increasing numbers of climate variables (dark red patches in Fig. 4). The prevalence of no-analogue climates is also a function of the requested precision of what constitutes a climate match (Fig. 3b). Here, we described the requested precision by the number of 'bins' of principal component scores. In a two-dimensional plot of the first two components, these can be visualized as rectangular areas with similar climate values in multivariate space. We find that there is initially a rapid increase in velocity values with increasing precision. Subsequently, the increase in estimated velocity values is monotonic, but no-analogue climates become more prevalent with increasing precision. We therefore find it useful to balance the precision of climate match against the prevalence of no-analogue climates (here we used 120 bins) to obtain general-purpose velocity maps.

In summary, climate change velocity estimates depend to some degree on user choices that include the methodological approach, the number of climate variables, the resolution of climate grids, and threshold settings of what constitutes a climate match. Yet, it is remarkable that the resulting maps of velocities are very robust in their overall ranking of exposure of organisms to climate change (compare Fig. 1 left vs. right, Fig. 2 insets, Fig. 1 vs. Fig. 4). There are virtually no changes to spatial arrangements of velocity values, except for the method-related differences that we have previously pointed out. We therefore propose that the approach should be useful for prioritizing conservation

and management prescriptions to address climate change.

Applications of forward and reverse velocities

The distance-based method proposed here can be implemented in two directions: a search of climate matches for a present cell in grids of projected future climate (as explained above), or the reverse search from a future reference cell to a climate match in a current grid (implemented by swapping the p and f vectors in the algorithms explained above). For the forward calculation we ask: what is the minimum distance an organism in the current landscape has to migrate to maintain constant climate conditions? Conversely, in the reverse calculation we ask: given the projected future climate habitat of a grid cell, what is the minimum distance an organism has to migrate from to colonize this climate habitat? The answers are not always similar, especially in mountainous terrain (Fig. 4).

Forward velocity calculations can be interpreted as the exposure of organisms to climate change. Low velocity values indicate that suitable habitat can be found nearby, and that is generally the case in areas of high topographic heterogeneity. The algorithm proposed in this paper also flags mountain-top positions as vulnerable (Figs 1 and 4a), and the extent of this vulnerability is a function of the absolute value of projected climate change, not just the rate per year. The forward calculation should therefore be particularly useful for the evaluation of protected area systems, or to assess the conservation status of species and their populations under climate change. Such assessments have been implemented using the slope-based velocity calculation (Ackerly *et al.*, 2010; Burrows *et al.*, 2011; IPCC, 2014; Schueler *et al.*, 2014) as well as using a climate-analogue approach not unlike the distance-based method developed here (Ordonez & Williams, 2013).

In the reverse calculation (Fig. 4b), the distance from future to modern habitat equivalents can be interpreted as a relative difficulty of species to colonize new habitat, or in the case of plants, the relative difficulty for populations to adapt *in situ* to new climate conditions supported by gene flow from matching populations. Notably, habitat near mountain tops is now evaluated as unproblematic habitat, because appropriately adapted organisms can be sourced from nearby downslope locations. Conversely, habitat in valley bottoms lacks nearby climate analogues, and organisms would have to travel much longer distances to colonize these locally new habitat conditions. Thus, the reverse velocity measure could be useful to prioritize human interventions through assisted migration, either in the context of rare species conservation (e.g., Richardson *et al.*, 2009), or imple-

mented as movement of locally adapted populations of wide-ranging species in regular reforestation operations (Gray *et al.*, 2011; Pedlar *et al.*, 2012).

We have previously noted that climate change velocities are a simple function of spatial and temporal variation in climate in a particular landscape. No biological data are used, and no specific biological response is inferred by the expected rate and direction of climate migrants. Consequently, we see value in combining climate change velocities with data on species' climate tolerances and adaptive capacities, or with statistical and mechanistic models of species' realized or fundamental niche spaces. For example, forward velocity calculations could be done with climate grids restricted to plant species distributions to evaluate pollen-flow among various locally adapted populations as a potential adaptive mechanism. For an assisted migration application, reverse velocities could be calculated between projected habitat and the current distribution to prioritize human intervention. In summary, the velocity of climate change measure complements but does not replace ecological modelling approaches for species vulnerability assessments and management applications.

Acknowledgements

We thank the Fulbright Program for a visiting scholar grant and the host David Ackerly at UC Berkeley for valuable discussions. This research is part of the AdapTree Project, funded by Genome Canada, Genome BC, Genome Alberta, Alberta Innovates Bio Solutions, the Forest Genetics Council of British Columbia, the BC Ministry of Forests, Lands and Natural Resources Operations, Virginia Tech, the University of British Columbia, and the University of California, Davis. Additional funding was provided by the Wilburforce foundation.

References

- Ackerly DD, Loarie SR, Cornwell WK, Weiss SB, Hamilton H, Branciforte R, Kraft NJB (2010) The geography of climate change: implications for conservation biogeography. *Diversity and Distributions*, **16**, 476–487.
- Burrows MT, Schoeman DS, Buckley LB *et al.* (2011) The pace of shifting climate in marine and terrestrial ecosystems. *Science*, **334**, 652–655.
- Burrows MT, Schoeman DS, Richardson AJ *et al.* (2014) Geographical limits to species-range shifts are suggested by climate velocity. *Nature*, **507**, 492–495.
- Corlett RT, Westcott DA (2013) Will plant movements keep up with climate change? *Trends in Ecology & Evolution*, **28**, 482–488.
- Diffenbaugh NS, Field CB (2013) Changes in ecologically critical terrestrial climate conditions. *Science*, **341**, 486–492.
- Dobrowski SZ, Abatzoglou J, Swanson AK, Greenberg JA, Mynsberge AR, Holden ZA, Schwartz MK (2013) The climate velocity of the contiguous United States during the 20th century. *Global Change Biology*, **19**, 241–251.
- Fordham DA, Wigley TML, Brook BW (2011) Multi-model climate projections for biodiversity risk assessments. *Ecological Applications*, **21**, 3317–3331.
- Gray LK, Gylander T, Mbogga MS, Chen PY, Hamann A (2011) Assisted migration to address climate change: recommendations for aspen reforestation in western Canada. *Ecological Applications*, **21**, 1591–1603.
- Hamann A, Wang TL, Spittlehouse DL, Murdock TQ (2013) A comprehensive, high-resolution database of historical and projected climate surfaces for Wes-

- tern North America. *Bulletin of the American Meteorological Society*, **94**, 1307–1309.
- IPCC (2014) Climate change 2014: impacts, adaptation and vulnerability. In: *Summary for Policy Makers*. Contribution of Working Group II to the Fifth Assessment Report of the Intergovernmental Panel on Climate Change (eds. Field CB, Barros VR, Dokken DJ, Mach KJ, Mastrandrea MD, Bilir TE, Chatterjee M, Ebi KL, Estrada YO, Genova RC, Girma B, Kissel ES, Levy AN, MacCracken S, Mastrandrea PR, White LL), pp. 1–32. Cambridge University Press, Cambridge, UK.
- IPCC (2007) Climate change 2007: the physical science basis. In: *Contribution of Working Group I to the Fourth Assessment Report of the Intergovernmental Panel on Climate Change* (eds Solomon S, Qin D, Manning M, Chen Z, Marquis M, Averyt KB, Tignor M, Miller HL), pp. 591–648. Cambridge University Press, Cambridge, UK.
- Loarie SR, Duffy PB, Hamilton H, Asner GP, Field CB, Ackerly DD (2009) The velocity of climate change. *Nature*, **462**, 1052–1055.
- Ordonez A, Williams JW (2013) Projected climate reshuffling based on multivariate climate-availability, climate-analog, and climate-velocity analyses: implications for community disaggregation. *Climatic Change*, **119**, 659–675.
- Pedlar JH, Mckenney DW, Aubin I *et al.* (2012) Placing forestry in the assisted migration debate. *BioScience*, **62**, 835–842.
- Richardson DM, Hellmann JJ, Mclachlan JS *et al.* (2009) Multidimensional evaluation of managed relocation. *Proceedings of the National Academy of Sciences of the United States of America*, **106**, 9721–9724.
- Sandel B, Arge L, Dalsgaard B, Davies RG, Gaston KJ, Sutherland WJ, Svenning JC (2011) The influence of late quaternary climate-change velocity on species endemism. *Science*, **334**, 660–664.
- Schueler S, Falk W, Koskela J *et al.* (2014) Vulnerability of dynamic genetic conservation units of forest trees in Europe to climate change. *Global Change Biology*, **20**, 1498–1511.
- Wang TL, Hamann A, Spittlehouse DL, Murdock TQ (2012) Climate WNA: high-resolution spatial climate data for western North America. *Journal of Applied Meteorology and Climatology*, **51**, 16–29.

Supporting Information

Additional Supporting Information may be found in the online version of this article:

Appendix S1. R code to calculate the distance from a grid cell with a climate value for the present to climate match in the future (forward calculation). This code is easiest to understand but fairly slow (about 5 h to process 1 million grid cells).

Appendix S2. R code to calculate the distance from a grid cell with a climate value for the present to climate match in the future (forward calculation). This code is more efficient using a rounding operation on the data to implement thresholds, and subsequently creating list of unique climate values with their climate matches (about 20 min to process 1 million cells).

Appendix S3. Multivariate extension of the R code shown in Appendix S2. This sample also uses a more efficient *k*-nearest neighbour search, and writes out source and target coordinates in a table for further analysis. The variables *p1* and *p2* represent principle components, but they could stand for any climate variable (about 5 min to process 1 million grid cells).

Appendix S4. Sample climate data at 1 km resolution for the geographic extent shown in Fig. 1 to run the code from Appendices S1–3.